HIGH-MOMENT – LOW-MOMENT DESCRIPTION OF MAGNETOVOLUME EFFECTS IN $Y(Mn_xAl_{1-x})_2$ AND $Y_xSc_{1-x}Mn_2$

M.E. GRUNER*and P. ENTEL

Theoretische Tieftemperaturphysik

Gerhard-Mercator-Universität Duisburg, D-47048 Duisburg, Germany

March 5, 2001

Abstract

Based on the assumption of a high-moment – low-moment instability of the Mn atom, we construct a simple spin model with coupled magnetic and spatial degrees of freedom to describe the Laves phase systems $Y(Mn_xAl_{1-x})_2$ and $Y_xSc_{1-x}Mn_2$. Monte Carlo simulations of this model qualitatively reproduce anomalies observed in these materials like a discontinuous giant volume change and anomalous thermal expansion behavior.

INTRODUCTION

Since more than hundred years, when Guillaume discovered the disappearance of thermal expansion in $Fe_{65}Ni_{35}$ around room temperature (Guillaume, 1897) widely known as *Invar effect*, magnetovolume effects have been in the center of many scientific research projects (for recent reviews on this field see: Wassermann, 1990; Shiga, 1994)).

An early explanation of this behavior has been given by Weiss with his phenomenological 2-γ-states model (Weiss, 1963). He assumed the existence of two distinct magnetic states of the iron atom: One at a large lattice constant and a high magnetic moment (HM) and another at a smaller lattice constant and a low magnetic moment (LM). Within the last decade this approach has gained some late support, since modern *ab initio* total energy calculations show that distinct minima exist on the binding surface at different volumes and magnetic moments with a difference in energy well within the reach of thermal excitation (e. g. Entel, Hoffmann, Mohn, Schwarz *et al.*, 1993; Schröter, Ebert, Akai, Entel *et al.*, 1995). Based on these results, the

*Corresponding author. Tel.: +49-203-379-3564, Fax.: +49-203-379-3665, eMail: me@thp.Uni-Duisburg.DE

authors performed Monte Carlo simulations of a Weiss type model, which allowed to reproduce some of the most striking anomalies of Fe-Ni alloys (Gruner, Meyer and Entel, 1998).

Apart from Fe-Ni alloys, magnetovolume effects have been discovered in a variety of different materials. One of the most exciting is the cubic Laves phase compound YMn_2. 20 years ago it was believed to be a Pauli paramagnet (Buschow and Sherwood, 1977), untill it was discovered that below 100 K the material undergoes a first order phase transition into an antiferromagnetic ground state structure with localized manganese moments (Nakamura, 1983; Shiga, Wada and Nakamura, 1983). The magnetic transition is accompanied by a discontinuous volume expansion of about 5 %, a huge moment increase and a large thermal hysteresis of about 20 K width. Also, a tetragonal lattice distortion of 0.5 % is observed (Cywinski, Kilcoyne and Scott, 1991). Above the phase transition the material shows an anomalously large thermal expansion of $\approx 50 \times 10^{-6}\,\mathrm{K}^{-1}$, which is referred to as *anti-Invar* behavior. Although only the manganese atoms carry a moment, the magnetic ground state structure is fairly complicated, because the manganese sublattice consists of four interconnected tetrahedra in which two of the six antiferromagnetic nearest neighbor bonds cannot be saturated (Fig. 1, left). In addition, it was found that this structure is helically modulated with a long period of 400 Å (Cywinski, Kilcoyne and Scott, 1991).

Moderate physical or chemical pressure leads quickly to a breakdown of the Mn moment. Under the external pressure of 3.3 kbar, antiferromagnetic order is not recovered down to very low temperatures (Oomi, Terada, Shiga and Nakamura, 1987; Kim-Ngan, Brommer, Franse and Hien, 1992; Mondal, Cywinski, H., Rainford *et al.*, 1992). The same effect is achieved by substituting 2 % of the Y atoms by Sc (Wada, Nakamura, Yoshimura, Shiga *et al.*, 1987b). The new ground state also has a much smaller lattice constant. On the other hand, if Mn is substituted by Al, the volume change becomes continuous and more Invar-like (Fig. 1, right). These observations together with low temperature data of several isostructural rare-earth-manganese compounds suggest that the Mn moments vanish if the Mn-Mn distance falls below a critical value (Wada, Nakamura, Fukami, Yoshimura *et al.*, 1987a).

In analogy to the Fe-Ni case, these facts are consistent with the assumption of a Weiss type high-moment low-moment instability of the Mn atom. This view gains further support from Mößbauer measurements of ^{119}Sn doped YMn_2. It can be seen from the hyperfine field distribution that at temperatures just below T_N magnetic and nonmagnetic Mn atoms coexist in the system (Block, Abd-Elmeguid and Micklitz, 1994). Accordingly, *ab initio* total energy calculations of YMn_2 show a two minima structure with small energy differences between the magnetic and nonmagnetic solutions (Asano and Ishida, 1988).

Therefore, the authors decided to apply a spin-1 Ising model with coupled spatial and magnetic degrees of freedom by means of Monte Carlo simulations. As in the Fe-Ni case, this model proves to be successful to repro-

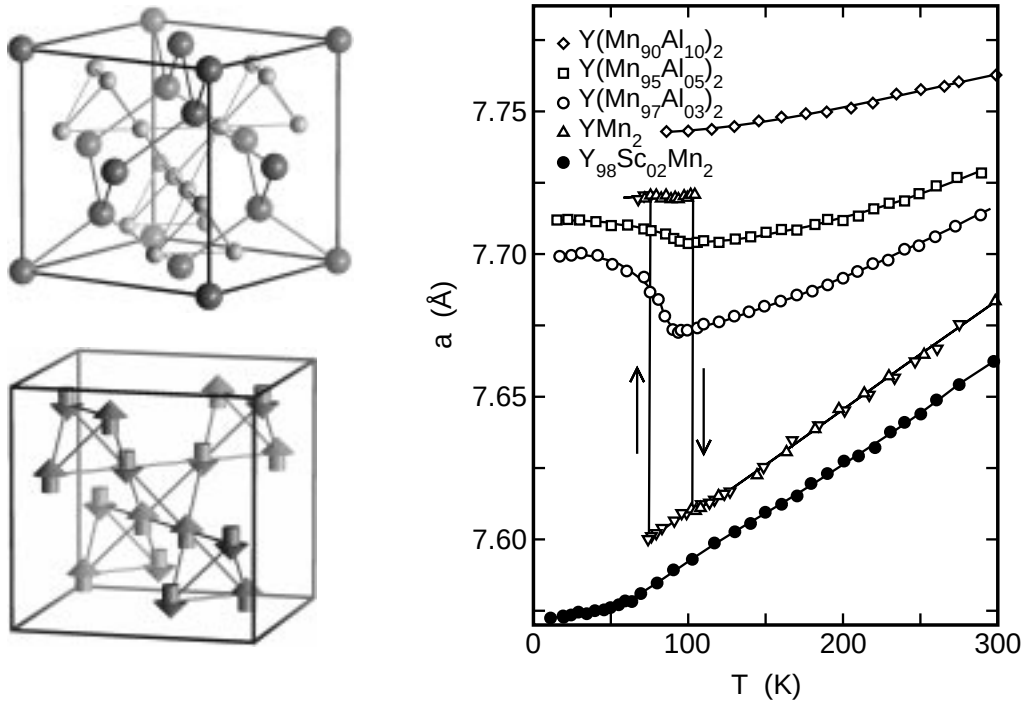

Figure 1: **Upper left:** C15 Laves phase structure of YMn_2. The larger spheres denote Y, the smaller ones Mn. **Lower left:** Collinear model of the antiferromagnetic structure of the Mn sublattice as proposed by Nakamura and Shiga (Nakamura, Shiga and Kawano, 1983). **Right:** Experimental lattice parameters of $Y(Mn_xAl_{1-x})_2$ and $Y_{98}Sc_{02}Mn_2$ (Shiga, Wada, Nakamura, Yoshimura *et al.*, 1987).

duce most of the magnetovolume anomalies observed in $Y_xSc_{1-x}Mn_2$ and $Y(Mn_xAl_{1-x})_2$.

THE WEISS TYPE MODEL

In order to incorporate magnetic as well as spatial degrees of freedom, we evaluate a spin-1 Ising model in combination with Lennard-Jones pair potentials at finite temperatures by means of Monte Carlo simulations. In contrast to previous simulations concerning this topic (Gruner and Entel, 1998), we consider the realistic binary C15 lattice structure as shown in Fig. 1. The different properties of atoms like Y, Mn, Sc and Al are accounted for by choosing different magnetic and elastic parameters depending on the types of atoms involved in the interaction. When studying ternary $Y_xSc_{1-x}Mn_2$ and $Y(Mn_xAl_{1-x})_2$ some Y atoms are randomly substituted by Sc atoms, and Mn by Al atoms, respectively. The interactions between the atoms are characterized by the following Hamiltonian:

$$H = \sum_i D_i S_i^2 + \sum_{<i,k>} J_{ik} S_i S_k + \sum_{<i,k>} V(r_{ik}, S_i, S_k). \qquad (1)$$

The discrete spin variables S_i can take the values $S_i = 0, \pm 1$ representing the LM and HM states of the Mn atoms, respectively. The first term introduces an energy difference between the atomic HM and LM states. The second one is the well known Ising Hamiltonian. It is necessary to calculate the double sum up to next nearest neighbor interactions, in order to stabilize the realistic spin structure shown in Fig. 1 (Terao, 1997). Since only Mn atoms are assumed to carry a moment, the first two terms are only evaluated if the involved lattice sites are occupied by Mn atoms. This means that only three free parameters are left: D_{Mn} is assigned a value of 1.1 mRy. The exchange constants are chosen as $J^{\mathrm{nn}}_{\mathrm{MnMn}} = 1.0\,\mathrm{mRy}$ and $J^{\mathrm{nnn}}_{\mathrm{MnMn}} = -0.25\,\mathrm{mRy}$ which give a reasonable value for the Néel temperature.

The last term characterizes the elastic properties as well as the coupling between magnetic and spatial degrees of freedom. In our simulations we use two sets of Lennard-Jones pair potentials, denoted HM and LM corresponding to the spin states of the interacting lattice sites:

$$V_{\mathrm{HM,LM}}(r_{ik}) = -4\,\epsilon^{AB}\left(\left(\frac{\sigma^{AB}_{\mathrm{HM,LM}}}{r_{ik}}\right)^{12} - \left(\frac{\sigma^{AB}_{\mathrm{HM,LM}}}{r_{ik}}\right)^{6}\right). \qquad (2)$$

Whether the interaction will be described by a HM or LM potential is decided by the spin state of the Mn atoms. If one of the interacting atoms is of the Mn type and in the S=0 state, the LM parameters are used, otherwise the HM parameters. Since HM potentials are chosen to prefer a larger spacing between the atoms than the LM potentials, the spin state of the Mn atoms is directly connected to the lattice volume. As mentioned before, these potentials also depend on the chemical elements involved in the interaction. This is necessary to stabilize the C15 structure of the compound as well as accounting for the different elastic properties of YAl_2 or $ScMn_2$. The distance between nearest neighbors in an ideal C15 compound with AB_2 stoichiometry is (in units of the lattice constant): $\sqrt{3}/4$ between two A atoms, $\sqrt{2}/4$ between two B atoms and $\sqrt{11}/8$ between atoms of type A and B. Since the minimum of the Lennard-Jones potential is located at a distance of $2^{1/6}\sigma^{\mathrm{AB}}$, this leads to $\sigma^{\mathrm{YY}} = 2.940$ Å, $\sigma^{\mathrm{MnMn}}_{\mathrm{LM}} = 2.391$ Å and $\sigma^{\mathrm{YMn}}_{\mathrm{LM}} = 2.804$ Å, in the case of for low moment YMn_2 with a T=0 lattice constant of 7.6 Å, that can be obtained from extrapolation of the experimental data. In order to agree with the measured lattice constant of the antiferromagnetic ground state we use $\sigma^{\mathrm{MnMn}}_{\mathrm{HM}} = 2.441$ Å and $\sigma^{\mathrm{YMn}}_{\mathrm{HM}} = 2.861$ Å. The experimental latice constant of YAl_2 at T=0 is 7.74 Å (Fig. 1), therefore we choose $\sigma^{\mathrm{AlAl}} = 2.477$ Å and $\sigma^{\mathrm{YAl}} = 2.904$ Å. Furthermore, we set $\sigma^{\mathrm{MnAl}}_{\mathrm{HM}} = \sigma^{\mathrm{MnAl}}_{\mathrm{LM}} = 2.486$ Å. The Sc atoms are considered to be about 10 % smaller than Y: $\sigma^{\mathrm{ScSc}} = 2.673$ Å, $\sigma^{\mathrm{YSc}} = 2.806$ Å, $\sigma^{\mathrm{MnSc}}_{\mathrm{HM}} = 2.601$ Å and $\sigma^{\mathrm{MnSc}}_{\mathrm{LM}} = 2.548$ Å. The ϵ^{AB} are the only parameters left which can be used for roughly adapting basic elastic properties like bulk modulus and thermal expansion. They obtain the values $\epsilon^{\mathrm{YY}} = \epsilon^{\mathrm{ScSc}} = \epsilon^{\mathrm{YSc}} = 60\mathrm{mRy}$, $\epsilon^{\mathrm{AlAl}} = \epsilon^{\mathrm{MnAl}} = 40\mathrm{mRy}$, $\epsilon^{\mathrm{YAl}} = \epsilon^{\mathrm{MnMn}} = 20\mathrm{mRy}$ and $\epsilon^{\mathrm{YMn}} = \epsilon^{\mathrm{ScMn}} = 10\,\mathrm{mRy}$.

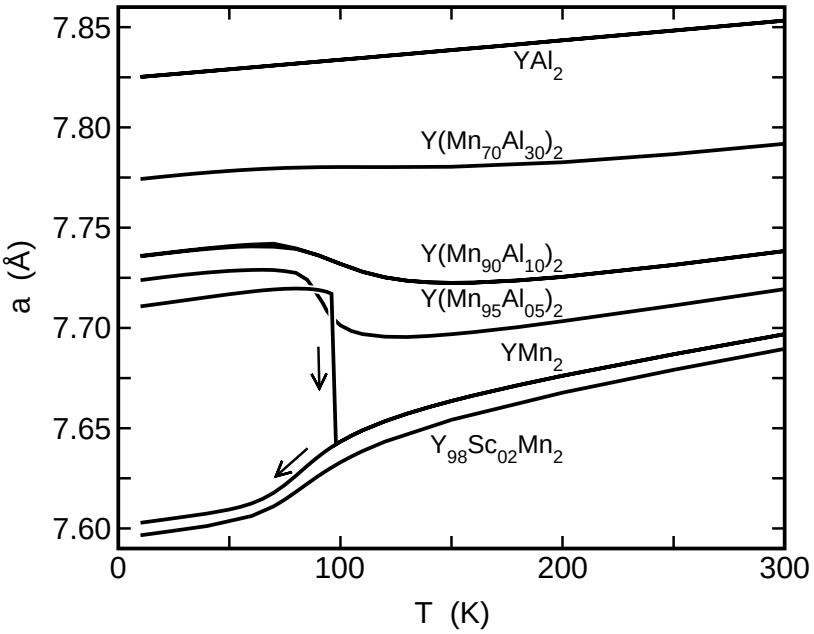

Figure 2: Calculated lattice parameters of $Y(Mn_xAl_{1-x})_2$ and $Y_{98}Sc_{02}Mn_2$.

As in our previous work, we use the standard isobaric Monte Carlo method (e. g. Allen and Tildesley, 1987) which allows for simulations in the canonical ensemble: For each lattice site we choose a new spin state $S_i \in \{0, \pm 1\}$, compute the energy difference and accept or reject the new state according to the Metropolis probability $\max(1, \exp(-\Delta H/T))$. Afterwards a new trial position is selected out of a cube around the old position. Again, the Metropolis criterion is used to decide whether the new position is accepted. In order to improve convergence, the size of the cube is given by the condition that about half of the propositions are to be accepted. After all atoms have been updated, the volume of the complete lattice is adapted by another Metropolis step. In this case, however, the difference in translational entropy must be taken into account, which is caused by the change of the volume from V to V'. This can be done by considering $\Delta\mathcal{H} = \Delta H - N\, k_\mathrm{B}\, T\, \ln(V'/V)$ when calculating the Metropolis probability.

The simulations were carried out on a C15 lattice with 12 288 atoms. For each temperature we performed 120 000 ... 480 000 lattice sweeps using the first 30 000 ... 120 000 for allowing the system to reach equilibrium before starting to evaluate the thermodynamical averages. The quantities are evaluated in the same way as described in Gruner, Meyer and Entel (1998).

THE RESULTS

Figure 2 presents the calculated lattice parameters and the averaged magnetic moment of the Mn atoms. In the case of pure YMn_2, we find upon heating a discontinuous volume decrease of the lattice parameter of 1 %, which is in good agreement with the experimental results shown in Fig. 1.

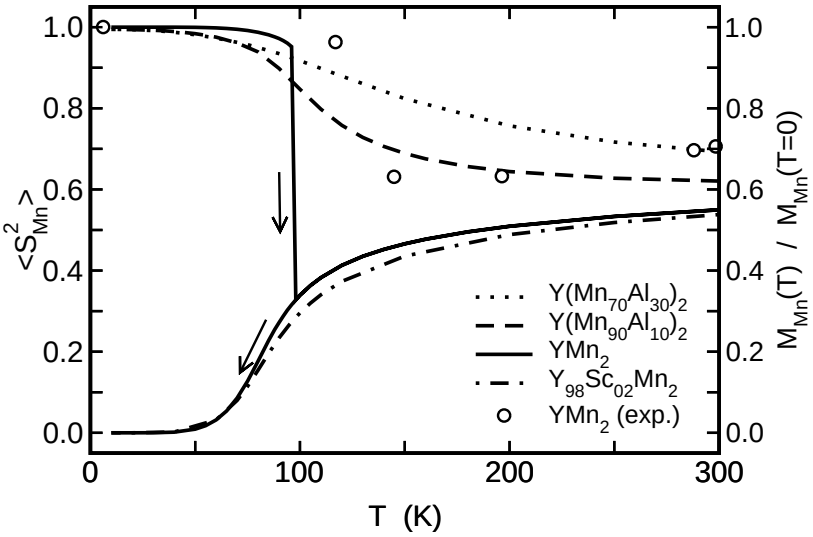

Figure 3: Calculated thermal average of the Mn moments. The experimental data were taken from neutron diffraction measurements: Motoya, Freltoft, Böni and Shirane (1988).

Accordingly, this decrease is accompanied by a collapse of the Mn moment to about one third of its low temperature value, which is well below the high-temperature limit. Consequently, further heating leads to a gradual increase of the mean Mn moments. This causes a pronounced enhancement of thermal expansion above T_{N} (Fig. 4), which is in our simulation even larger than in the experiment. Upon cooling down, the system does not jump back to the antiferromagnetic high volume state, but continues decreasing the Mn moment and ends up in a nonmagnetic state at a lower volume. As can be seen from Fig. 5, this state is higher in energy and therefore metastable. A similar behavior can be found for Sc doped YMn_2. Here, the nonmagnetic state is lower in energy due to the reduced lattice constant caused by the smaller Sc.

The thermal asymmetry of the first order HM-LM transition in pure YMn_2 must be considered as an artefact of the standard Monte Carlo method used in our simulations. Upon heating the transition from the HM to the LM phase is supported by the erosion of antiferromagnetism by spin fluctuations and thermal excitation of LM states. In the overheated system a continuously increasing number of LM atoms lead to a continuously decreasing lattice constant until the system reaches thermal equilibrium again. Upon cooling, however, the transition requires a complicated magnetic structure to be established and a huge volume jump to happen at the same time. Since our algorithm allows only for consecutive spin and volume changes and the intermediate states my be prohibitively high in energy, such an event is very unlikely to occur in a typical simulation time. A solution for this problem can be a global update scheme allowing for a simultaneous change of the spin state and volume of the simulation cell. The difficulty with such

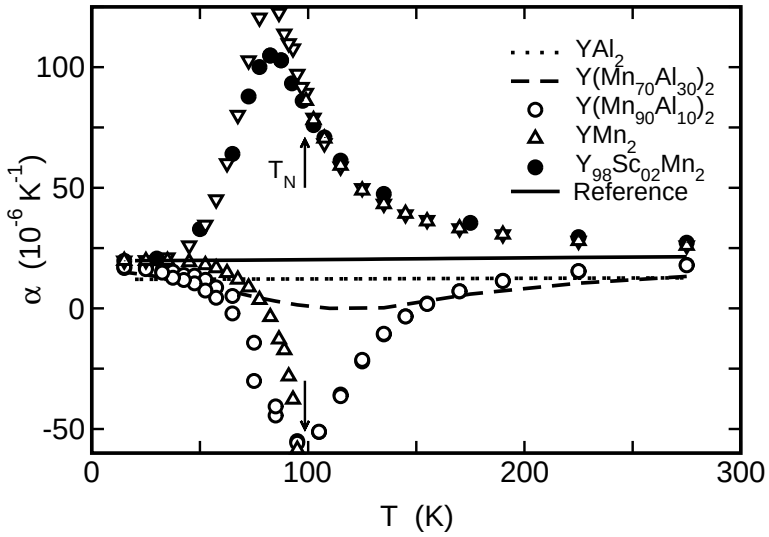

Figure 4: Calculated thermal expansion coefficient of $Y(Mn_xAl_{1-x})_2$ and $Y_{98}Sc_{02}Mn_2$. For pure YMn_2, values obtained during heating are denoted by triangles pointing upwards, whereas triangles pointing downwards mark the data points for decreasing temperatures.

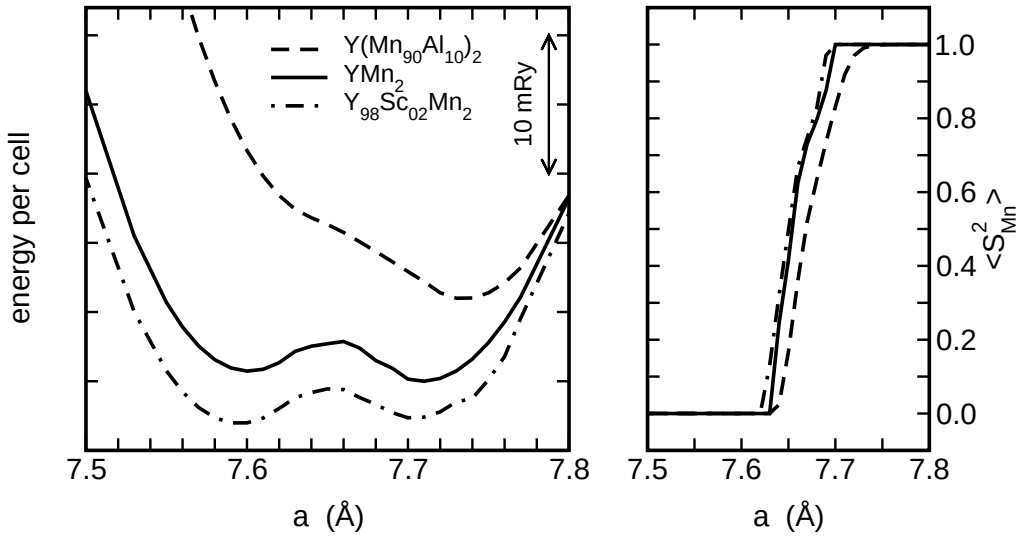

Figure 5: Internal energy and magnetic moment as a function of the lattice constant at $T = 4\,\mathrm{K}$.

an approach is that it easily produces too large energy differences between the proposed states which lead to vanishing acceptance probabilities. Furthermore, it should fulfill the *detailed balance* condition in order to guarantee thermal equilibrium to be reached in the long run. To find an efficient scheme that meets these requirements is subject to future work.

Replacement of a few at-% Mn by Al causes a general expansion of the lattice. Since Al does not possess a low volume state, collective switching of the Mn atoms to the nonmagnetic state is connected with lattice distortions which raise the energy of the metastable LM phase. As a consequence, the

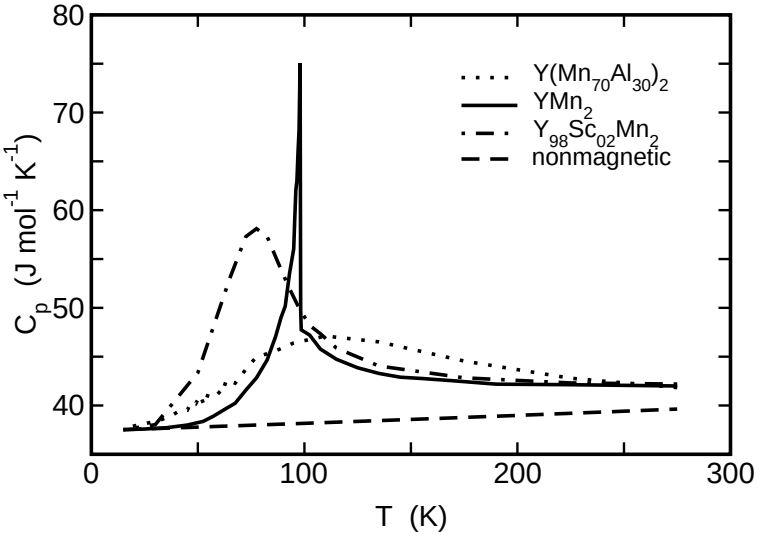

Figure 6: Calculated specific heat of $Y(Mn_{70}Al_{30})_2$, YMn_2, $Y_{98}Sc_{02}Mn_2$ and a reference system without magnetic interactions. In the case of YMn_2 only the values of the heating procedure are shown.

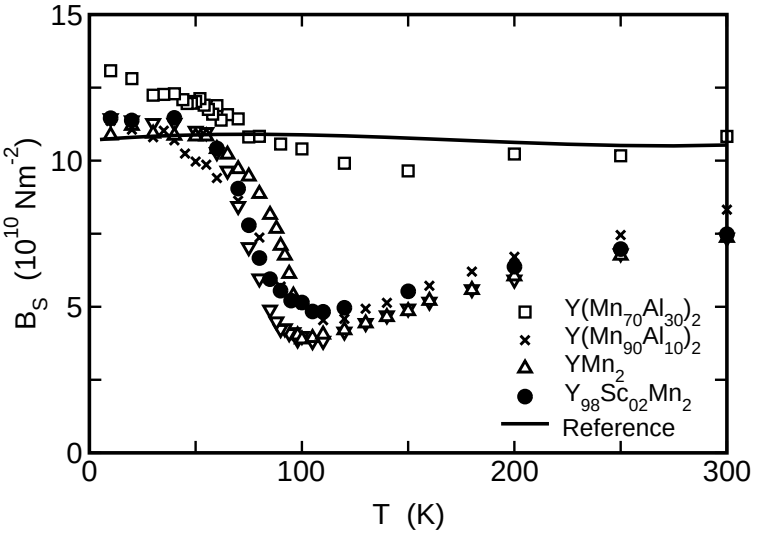

Figure 7: Calculated adiabatic bulk modulus.

first order transition vanishes and the average of the Mn moments decrease continuously with increasing temperature. This causes a reduction of thermal expansion, which is typical for Invar materials, in contrast to the anti-Invar behavior of YMn_2 and $Y_xSc_{1-x}Mn_2$.

The specific heat C_p of YMn_2 (Fig. 6) shows a sharp anomaly at T_N as can be expected for a first order transition. We omitted results for decreasing temperatures since they are very similar to those obtained for $Y_{98}Sc_{02}Mn_2$. At this composition, we find a huge Schottky anomaly around 70K, which coincides with the maximum of the thermal expansion coefficient and is caused by thermal excitation of magnetic Mn states. The smeared out maximum of C_p in $Y(Mn_{70}Al_{30})_2$ has almost the same origin: In this case, a Schottky

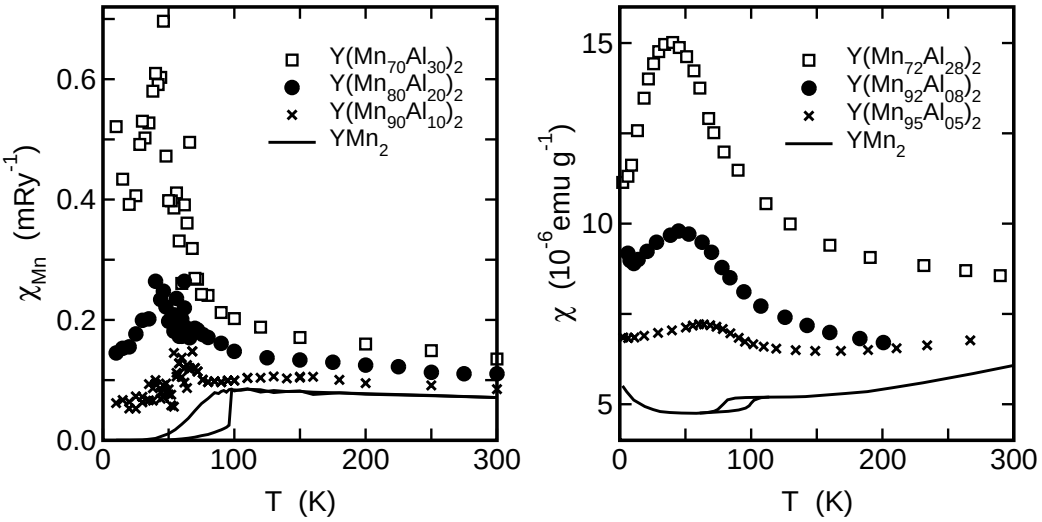

Figure 8: **Left:** Calculated Susceptibility of $Y(Mn_xAl_{1-x})_2$. **Right:** Experimental Susceptibility of $Y(Mn_xAl_{1-x})_2$ at an external field of 8.5 kOe: Shiga, Wada, Nakamura, Yoshimura *et al.* (1987).

anomaly occurs around 120 K that is caused by thermal excitation of LM atoms in a mainly magnetic environment. Common to all systems is a considerable enhancement of the specific heat at higher temperatures compared to a hypothetical nonmagnetic material, which is in agreement with experimental findings of Imai, Wada and Shiga (1995). Contrary to our results, a comparable Schottky anomaly has not been observed in $Y_{98}Sc_{02}Mn_2$. Instead, experiments show an increase of C_p above 200 K. This means that the simulated Schottky anomaly should be located at higher temperatures and therefore the fit of our model parameters is not optimal. In order to improve this, new parameters must be introduced, like weighting factors for HM and LM states that take care of entropy differences between them. So far, these have been left out for the sake of simplicity. The adiabatic bulk modulus of YMn_2 (Fig. 7) is reduced drastically around the transition temperature in typical fashion for materials with magnetovolume effects. This behavior does not change significantly upon doping with Sc or with up to 10 % Al.

The comparison between the calculated and measured susceptibilities (Fig. 8) shows a remarkable agreement, although the calculation were performed without magnetic field in contrast to a field of 8.5 kOe applied in the experiment. This indicates that an AF to spin glass transition which supposedly happens with increasing Al content can be well described by the magnetic part of our Hamiltonian. This is not really a surprise, since diluted lattices with frustrated interactions, as is the case in the Mn sublattice, have a tendency to become spin glasses (Villain, 1979). However, to shed more light on this issue, the calculations should be repeated using a spin-only Hamiltonian, since the elastic interactions are not expected to play an important role in this respect. This would allow for better statistics by choosing a longer simulation time as well as for field cooled and zero field cooled cycles to be

performed.

CONCLUSION

Within the framework of our model we are able to calculate the thermodynamic behavior of $Y(Mn_xAl_{1-x})_2$ and $Y_xSc_{1-x}Mn_2$ in qualitative agreement with the experiment. Although quantitative agreement is not achieved, we see the same tendencies upon variation of temperature or composition. Especially to mention in this respect are the vastly enhanced thermal expansion in pure YMn_2, the vanishing of the first order transition when exchanging Y by Sc or Mn by Al, and the enhancement of the specific heat above T_N.

In contrast to the experimental data, we do not see a reduction of the low temperature lattice constant compared to pure YMn_2 at small Al concentrations ($\leq 5\,\%$). This effect may well be connected with the tetragonal distortion of the lattice at low temperatures and the noncollinearity of the spin structure in YMn_2. In this case we cannot expect to see this effect in our calculations, since our model would have to extended to include Heisenberg spins and non-isotropic volume changes.

Probably the most important aspect of our simulations is, that we are able to explain Invar and anti-Invar behavior with one and the same mechanism, a HM-LM instability of the transition metal atom, supporting the view that both effects are closely related and possibly of the same origin.

References

Allen, M. P. and D. J. Tildesley (1987). *Computer Simulation of Liquids*. Clarendon, Oxford.

Asano, S. and S. Ishida (1988). Electronic structure of Laves phase compounds. *J. Magn. Magn. Mater* **70**, 39.

Block, A., M. M. Abd-Elmeguid and H. Micklitz (1994). Nature of the pressure-induced magnetic phase transition in the itinerant-electron antiferromagnet YMn_2: A microscopic view. *Phys. Rev. B* **49**, 12365.

Buschow, K. H. J. and R. C. Sherwood (1977). Magnetic properties and hydrogen absorption in rare-earth intermetallics of the type RMn_2 and R_6Mn_{23}. *J. Appl. Phys.* **48**, 4643.

Cywinski, R., S. H. Kilcoyne and C. A. Scott (1991). Magnetic order and moment stability in YMn_2. *J. Phys.: Cond. Mat.* **3**, 6473.

Entel, P., E. Hoffmann, P. Mohn, K. Schwarz *et al.* (1993). First-principles calculations of the instability leading to the Invar-effect. *Phys. Rev. B* **47**, 8706.

Gruner, M. E. and P. Entel (1998). Monte carlo simulations of magnetovolume instabilities in anti-invar systems. *Comp. Mat. Sci.* **10**, 230.

Gruner, M. E., R. Meyer and P. Entel (1998). Monte Carlo simulations of high-moment – low-moment transitions in Invar alloys. *Eur. Phys. J. B* **2**, 107.

Guillaume, C.-E. (1897). Recherches sur les aciers au nickel. Dilatations aux températures élevées; résistance électrique. *C. R. Acad. Sci.* **125**, 235.

Imai, H., H. Wada and M. Shiga (1995). Effects of spin fluctuations on the specific heat in YMn_2 and $Y_{0.97}Sc_{0.03}Mn_2$. *J. Phys. Soc. Jpn.* **64**, 2198.

Kim-Ngan, N. H., P. E. Brommer, J. J. M. Franse and T. D. Hien (1992). Effect of pressure on the néel temperature of YMn_2. *Physica B* **179**, 231.

Mondal, S., R. Cywinski, K. S. H., B. D. Rainford *et al.* (1992). Pressure dependence of the magnetic order in YMn_2 and $TbMn_2$. *Physica B* **180-181**, 108.

Motoya, K., T. Freltoft, P. Böni and G. Shirane (1988). Neutron scattering study of spin fluctuations in $Y(Mn_{1-x}Al_x)_2$. *Phys. Rev. B* **38**, 4796.

Nakamura, Y. (1983). Magnetovolume effects in Laves phase intermetallic compounds. *J. Magn. Magn. Mater* **31-34**, 829.

Nakamura, Y., M. Shiga and S. Kawano (1983). Antiferromagnetism of YMn_2 intermetallic compound. *Physica* **120B**, 212.

Oomi, G., T. Terada, M. Shiga and Y. Nakamura (1987). Effect of pressure on the Néel temperature of the intermetallic compound YMn_2. *J. Magn. Magn. Mater* **70**, 137.

Schröter, M., H. Ebert, H. Akai, P. Entel *et al.* (1995). First-principles investigations of atomic disorder effects on magnetic and structural instabilities in transition-metal alloys. *Phys. Rev. B* **52**, 188.

Shiga, M. (1994). Invar alloys. In R. W. Cahn, P. Haasen and E. J. Kramer, editors, *Materials Science and Technology*, volume 3B, chapter 10, 159. VCH, Weinheim. Volume editor: Buschow, K. H. J.

Shiga, M., H. Wada, H. Nakamura, K. Yoshimura *et al.* (1987). Characteristic spin fluctuations in $Y(Mn_{1-x}Al_x)_2$. *J. Phys. F: Met. Phys.* **17**, 1781.

Shiga, M., H. Wada and Y. Nakamura (1983). Magnetism and thermal expansion anomaly of RMn_2 (R = Y, Gd, Tb, Ho and Er). *J. Magn. Magn. Mater* **31-34**, 119.

Terao, K. (1997). The spin configuration in antiferromagnetic YMn_2 with the cubic Laves phase (C15) structure. *J. Phys. Soc. Jpn.* **66**, 1796.

Villain, J. (1979). Insulating spin glasses. *Z. Phys. B* **33**, 31.

Wada, H., H. Nakamura, E. Fukami, K. Yoshimura *et al.* (1987a). Spin fluctuations of $Y(Mn_{1-x}Al_x)_2$ and $Y_{1-x}Sc_xMn_2$. *J. Magn. Magn. Mater* **70**, 17.

Wada, H., H. Nakamura, K. Yoshimura, M. Shiga *et al.* (1987b). Stability of Mn moments and spin fluctuations in RMn_2 (R:rare earth). *J. Magn. Magn. Mater* **70**, 134.

Wassermann, E. F. (1990). Invar: Moment-volume instabilities in transition metals and alloys. In K. H. J. Buschow and E. P. Wohlfahrt, editors, *Ferromagnetic Materials*, volume 5, chapter 3, 237. Elsevier, Amsterdam.

Weiss, R. J. (1963). The origin of the Invar effect. *Proc. Phys. Soc.* **82**, 281.